# A Flight-to-Ground Mapping Strategy to Reproduce Entry Trajectory Conditions in ICP Facilities

Presented by: Andrea Scaboro


**Andrea Scaboro** *(University of Illinois Urbana-Champaign)*
Massimo Franco, Alessandro Meini, Teddy Mansfield, Francesco Panerai, Gregory Elliott *(University of Illinois Urbana-Champaign)*
Daniele Boncompagni *(SpaceX)*
Marco Panesi *(UC Irvine)*

**Thermal & Fluids Analysis Workshop 2025**
**NASA Ames Research Center**

San Jose, CA
August 4-7, 2025

# Outline

- Introduction
- Experimental Methods
- Physical Modeling
- Numerical Methods
- Methodology
- Results
- Conclusions

# Introduction

*Credits to SpaceX*
*https://www.youtube.com/watch?v=j2BdNDTlWbo&t=1s&ab_channel=SpaceX*

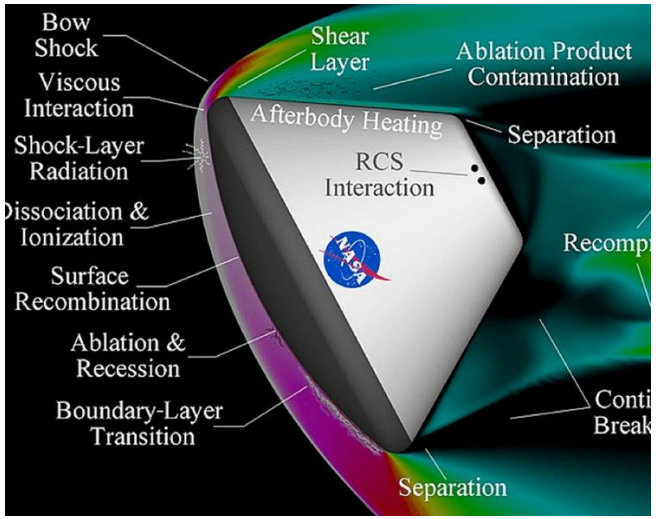


*Credits to NASA*

High speed vehicles **re-entry** from orbit into the planetary atmosphere

A **bow shock** forms in front of the body

After the shock the kinetic energy quickly converts into thermal energy

This leads to high heat rates that are experienced at the surface of high-speed entry vehicles

*https://spaceflightnow.com/2022/05/24/spacex-swapping-heat-shield-for-next-crew-mission-due-to-manufacturing-defect/*

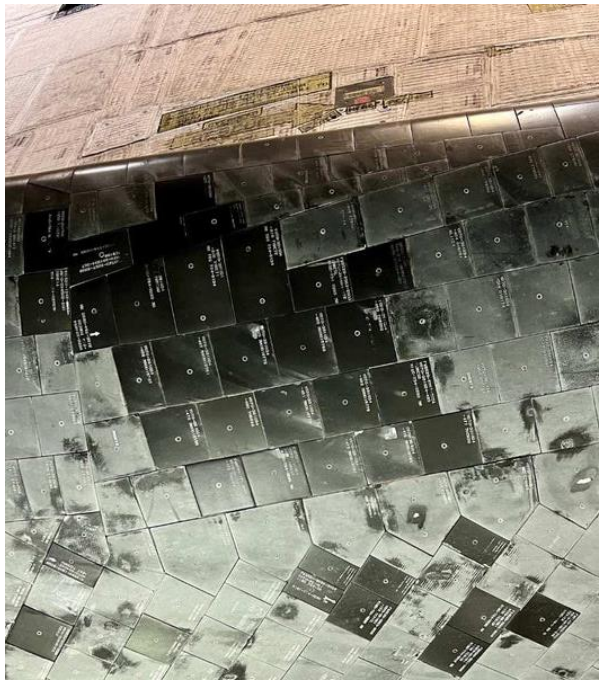

*https://astronautfoods.com/blogs/news/where-is-the-space-shuttle-endeavour?srsltid=AfmBOorodJislym4K5p-5a7sBYV9of-OD_mT_uePOiKQ-mIUXMvku4Pv*

# Introduction

To protect these vehicles, **Thermal Protection Systems (TPS)** are used

These TPS can be made of **refractory materials** (e.g., ceramics) or **ablative materials**

In order to ground test these different TPS that are going to be used to protect the flying vehicle during re-entry, **high-enthalpy facilities** are used

These facilities can be:

- **Arc Jet Facilities**
- **Inductively Coupled Plasma (ICP) Facilities**

# Experimental Methods

PLASMATRON X FACILITY

University of Illinois Urbana-Champaign

Center for Hypersonics & Entry Systems Studies (CHESS)

- Radiofrequency (RF) ICP torch applying 2.1 MHz excitation to an induction coil
- **Coil power** from 13.5 kW to 350 kW
- Various **gases** such as air, carbon dioxide, etc.
- Precisely controlled **chamber pressure**
- Probe mounted on a rotary arm

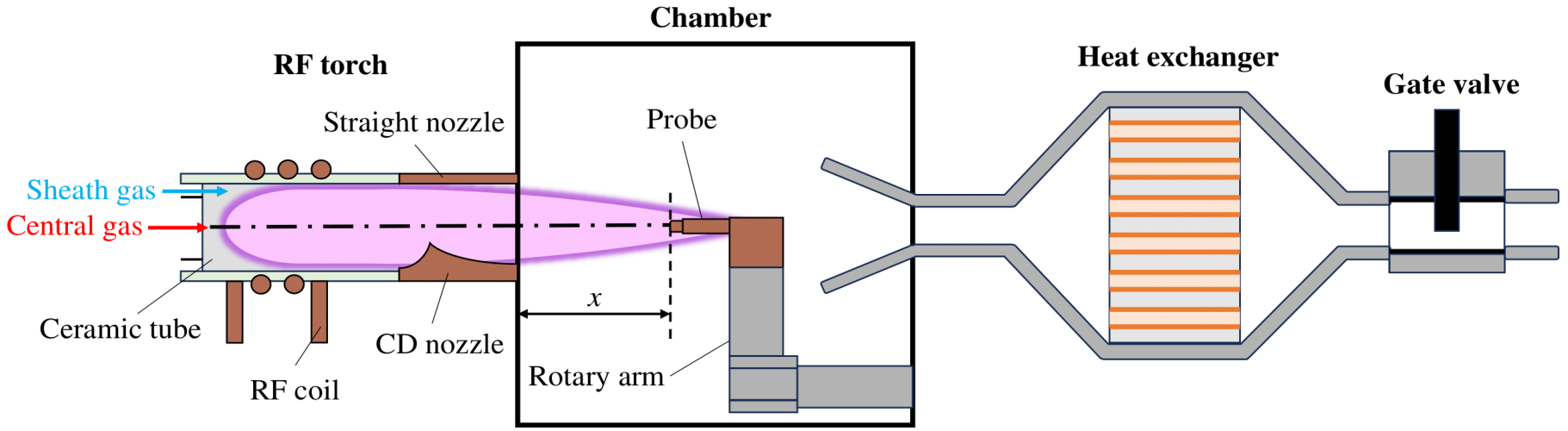


*Credits to Massimo Franco for the scheme*

# Experimental Methods

## PLASMATRON X FACILITY

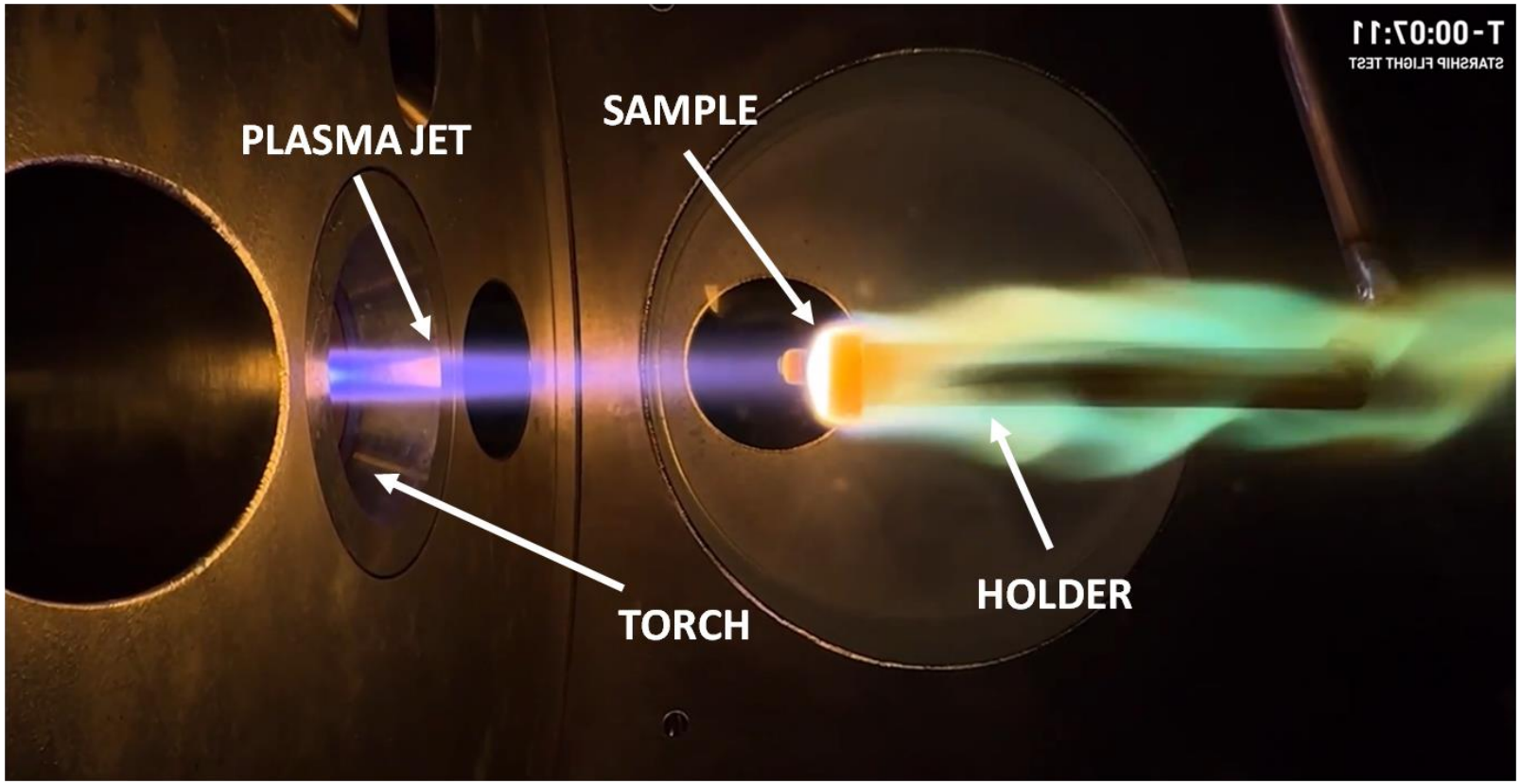


*Credits to SpaceX (*https://x.com/SpaceX/status/1857841326542434339?lang=en)

# Experimental Methods

**Optical Emission Spectroscopy (OES)** data were collected:

- Teledyne IsoPlane SCT-320 **spectrometer**
- 600 grooves/mm grating
- Wavelength range of approximately 130 nm
- Measurements taken both axially and radially along the stagnation line

Different **probes** can be used:

- Test coupon with **pyrometer**
- Slug **calorimeter**
- **Pitot probe**

TO MEASURE

- **Hot wall temperature**
- **Cold wall heat flux**
- **Dynamic pressure**


*https://www.imagesspa.it/teledyne-princeton-instruments-isoplane-spectrometer-isoplane-320*

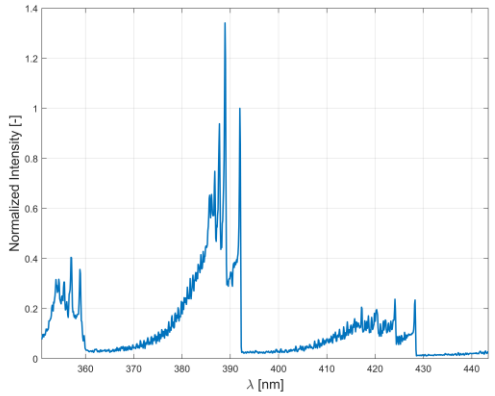


*Example of an experimental spectra after calibration*

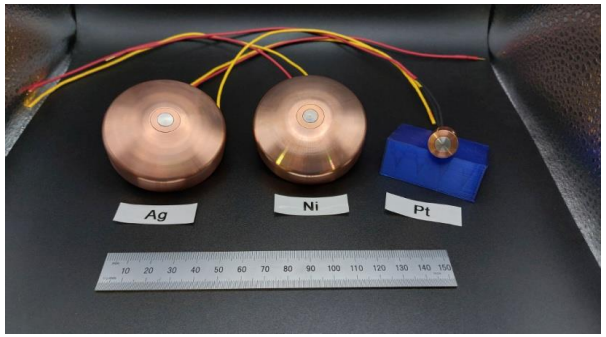


*Different calorimeter coatings (credits to M. Franco)*

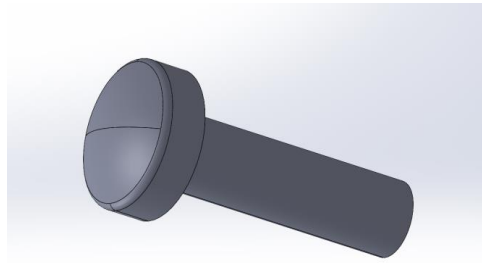

*3D model of the sample probe (credits to M. Franco)*

# Physical Modeling

## PLASMA FIELD and ELECTROMAGNETIC FIELD

Assumptions:

- Chemical and thermodynamic **non-equilibrium**
- **Two-temperature** model ($T_h$ and $T_v$)
- Plasma is a mixture of neutral and charged species
- Plasma assumed to be **quasi-neutral** and **collision-dominated**
- **Thermodynamics**, **transport**, and collisional-radiative **kinetics** from the PLATO library
- Electromagnetic field described by **Maxwell's equations**, with low-frequency, low magnetic Reynolds number, and ambipolar diffusion approximations

Mass continuity equations for each species, momentum equations, heavy-particle energy equation, and vibrational energy equation are formulated as:

$$\frac{\partial \rho_s}{\partial t} + \nabla \cdot [\rho_s (\mathbf{v} + \mathbf{U}_s)] = \dot{\omega}_s, \quad s \in \mathcal{S},$$

$$\frac{\partial \rho \mathbf{v}}{\partial t} + \nabla \cdot (\rho \mathbf{v}\mathbf{v} + p\mathbf{I}) = \nabla \cdot \boldsymbol{\tau} + \mathbf{J} \times \mathbf{B},$$

$$\frac{\partial \rho E}{\partial t} + \nabla \cdot (\rho H \mathbf{v}) = \nabla \cdot (\boldsymbol{\tau}\mathbf{v} - \mathbf{q}) + \mathbf{J} \cdot \mathbf{E}',$$

$$\frac{\partial \rho_e e_{ve}}{\partial t} + \nabla \cdot (\rho_e e_{ve} \mathbf{v}) = -\nabla \cdot \mathbf{q}_{ve} - p_e \nabla \cdot \mathbf{v} + \Omega^c_{ve} + \mathbf{J} \cdot \mathbf{E}'.$$

The energy exchange term in the vibrational energy equation is described by the following contributions:

$$\Omega^c_{ve} = \Omega^{\mathrm{VT}} + \Omega^{\mathrm{TE}} + \Omega^{\mathrm{DE}} + \Omega^{\mathrm{IE}} + \Omega^{\mathrm{CV}} + \Omega^{\mathrm{CEL}}$$

# Physical Modeling

## PROBE BOUNDARY CONDITIONS

The mass flux source term at the probe is strongly influenced by wall reactions

CATALYSIS:

**Heat flux <u>at the wall</u>** is strongly affected by **catalytic** reactions:

$N + N \longrightarrow N_2$
$O + O \longrightarrow O_2$

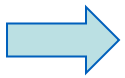

**Recombination reactions**

- Recombination reactions are strongly **exothermic**
- Reactions are described by the recombination probability **γ**

## RECOMBINATION PROBABILITY **γ :**

Surface property that quantifies the likelihood that an atom or ion striking a surface will recombine with another particle to form a molecule

How to determine the **recombination probability**?

- Literature
- Full ICP finite-rate chemistry simulations
- 1D boundary layer rebuilding

The conditions of interest are:

- **Non-catalytic** wall (γ = 0)
- **Fully catalytic** wall (γ = 1)
- **Copper catalytic** wall (0.01 < γ < 0.1)

# Numerical modeling

## PLASMA SOLVER:

- Using the structured finite-volume solver **HEGEL** (HighfidElity tool for maGnEtogas-dynamic appLications)
- Using the **PLATO** library for the computation of plasma thermodynamic and transport properties
- Inviscid fluxes evaluated through the **AUSM+up** scheme
- **MUSCL** reconstruction procedure
- Time integration using **Backward Euler (BE)** scheme

## ELECTROMAGNETIC SOLVER:

- Equations solved using the mixed finite element solver **FLUX**
- Weak-form formulations for both time-domain and frequency-domain problems implemented in **FLUX** using **MFEM**

## COUPLING OF HEGEL, PLATO, AND FLUX:

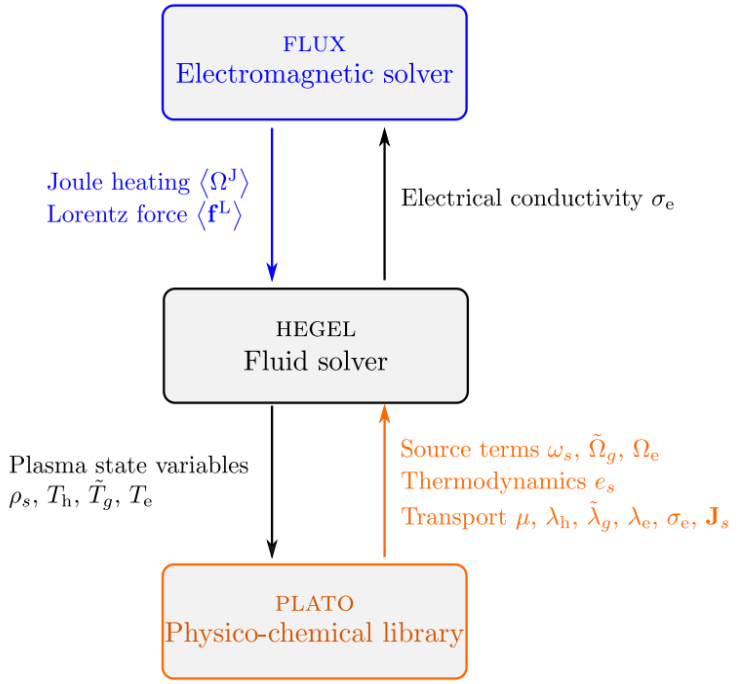


*Credits to S. Kumar*

# Physical Modeling

## STAGNATION LINE 1D FLOW

- Methodology proposed by **Klomfass and Müller** for stagnation line flow
- Quasi-one-dimensional approximation of the **stagnation streamline**
- The resulting set of simplified equations is called the **Dimensionally Reduced Navier–Stokes Equations (DRNSE)**

$$\bar{\mathbf{u}}_{,t} + \bar{\mathbf{F}}^I_{,r} + \bar{\mathbf{F}}^V_{,r} + \left(\bar{\mathbf{G}}^I + \bar{\mathbf{G}}^V\right) r^{-1} = \mathbf{S},$$

$$\bar{\mathbf{u}} = \begin{bmatrix} \rho_1 \\ \vdots \\ \rho_N \\ \rho\bar{v}_r \\ \rho\bar{v}_\theta \\ \rho E \end{bmatrix}, \quad \bar{\mathbf{F}}^I = \begin{bmatrix} \rho_1\bar{v}_r \\ \vdots \\ \rho_N\bar{v}_r \\ \rho\bar{v}_r^2 + p \\ \rho\bar{v}_r\bar{v}_\theta \\ \rho\bar{v}_r H \end{bmatrix}, \quad \bar{\mathbf{F}}^V = \begin{bmatrix} j_{r1} \\ \vdots \\ j_{rN} \\ \tau_{rr} \\ \tau_{r\theta} \\ q_r + \tau_{rr}\bar{v}_r \end{bmatrix},$$

# Numerical Modeling

- Based on the methodology proposed by **Klomfass** and is integrated within the **HEGEL** and **PLATO** frameworks
- Inviscid fluxes evaluated using the **ROE** scheme

$$\bar{\mathbf{G}}^I = \begin{bmatrix} 2\rho_1(\bar{v}_r + \bar{v}_\theta) \\ \vdots \\ 2\rho_N(\bar{v}_r + \bar{v}_\theta) \\ 2\rho\bar{v}_r(\bar{v}_r + \bar{v}_\theta) \\ 3\rho\bar{v}_\theta(\bar{v}_r + \bar{v}_\theta) - 2\bar{p} \\ 2\rho H(\bar{v}_r + \bar{v}_\theta) \end{bmatrix}, \quad \bar{\mathbf{G}}^V = \begin{bmatrix} 2j_{r1} \\ \vdots \\ 2j_{rN} \\ 2(\tau_{rr} - \bar{\tau}_{\theta\theta} + \bar{\tau}_{r\theta}) \\ -\bar{\tau}_{\theta\theta} + 3\bar{\tau}_{r\theta} \\ 2(q_r + \bar{\tau}_{rr}\bar{v}_r + \bar{\tau}_{r\theta}\bar{v}_r + \bar{\tau}_{\theta\theta}\bar{v}_\theta) \end{bmatrix}$$

# Methodology

## PROCEDURE:

1. Test the **TPS samples** under specified conditions in the ICP facility
2. Use **diagnostic tools**, specifically the slug calorimeter and OES, to measure heat flux on the probe and plasma emission
3. Run several **simulations** to obtain a detailed description of the plasma field in the ICP
4. Use experiments to **validate** the numerical model
5. Extract relevant flow quantities from the simulations to extrapolate the test conditions to **flight conditions**

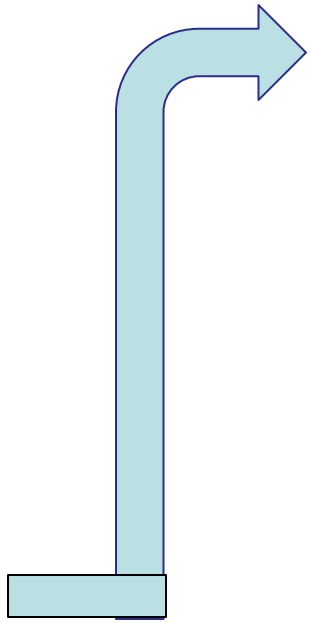

## FLIGHT EXTRAPOLATION:

The extrapolation is done using the **Local Heat Transfer Simulation (LHTS)** technique

According to LHTS, matching the ICP probe **boundary layer** to the flying body boundary layer allows reproduction of flight condition on the ground

This can be done by matching the **heat flux** in flight and on the ground, achievable by matching 3 key parameters:

- Boundary layer edge **stagnation enthalpy $H_e$**
- Boundary layer edge **stagnation pressure $P_e$**
- Boundary layer edge **radial gradient of the radial velocity $dU_e/dr$**

# Methodology

## CONDITIONS MATRIX:

| | Full ICP Simulations | 1D Stag Line Simulations | Experiments (heat flux + OES) |
|---|---|---|---|
| **Pressure [mbar]** | 70 | 50 to 260 | 50 to 256 |
| **Power [kW]** | 50-100-150-200-250 | 50 to 250 | 50 to 250 |

- The gas considered was **AIR** (78.084% $N_2$, 20.946% $O_2$, 0.934% Ar, 0.0414% $CO_2$)
- **Mass flow rate** was fixed at 6 g/s
- **Probes** considered were isoQ 30 to 60 mm (no significant change was observed in the measured heat flux)
- The calorimeter used was made of **copper**

# Methodology

## FULL ICP SIMULATIONS:

Full ICP simulations were performed reproducing the whole physics happening inside the Plasmatron X facility.

After several tests, the more accurate simulations required the following **setup**:

- **2D axisymmetric** domain
- **NLTE** simulations using Air11 and a two-temperature model
- **Time-accurate** solution (the flow is unsteady)
- For copper, the **recombination probability** was set to 0.01
- 2nd order **MUSCL** reconstruction
- Inviscid fluxes computed with the **AUSM+up** scheme

## COMPUTATIONAL DOMAIN:

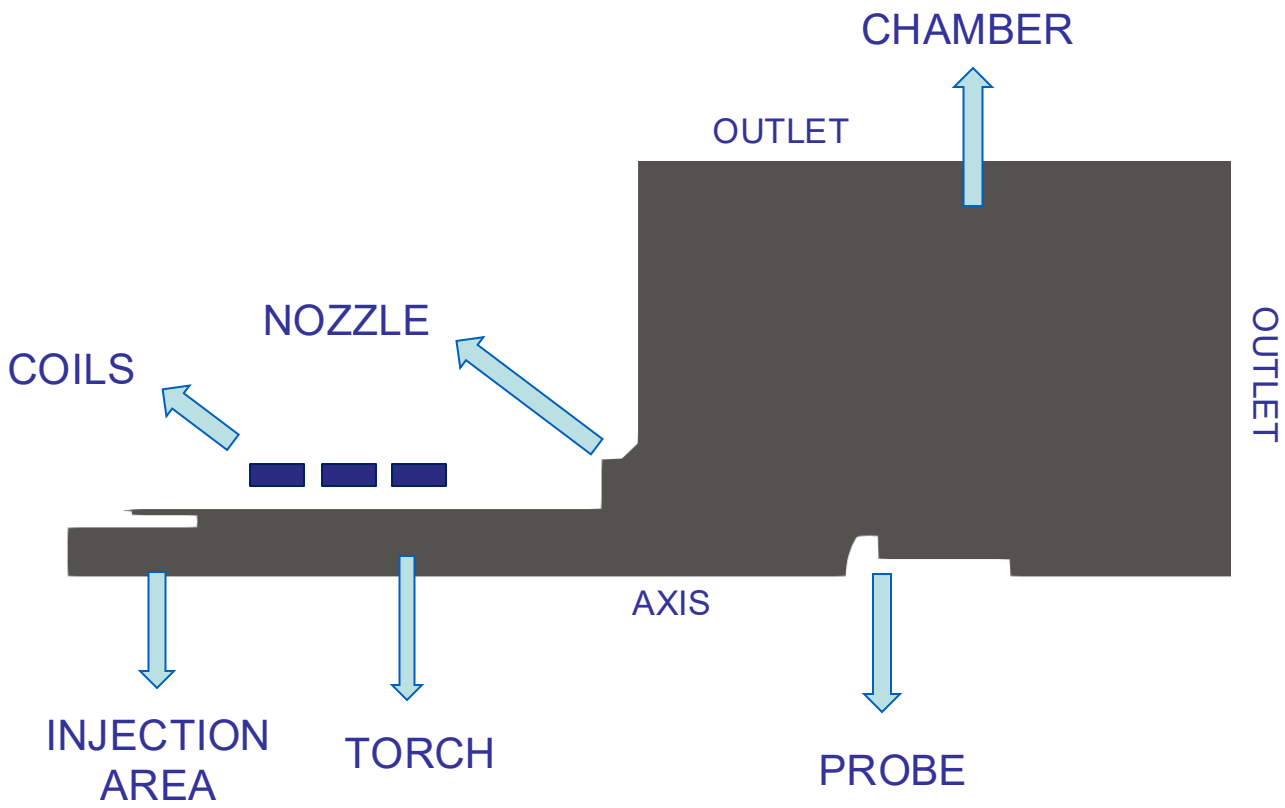

# Results

## FULL ICP SIMULATION RESULTS:

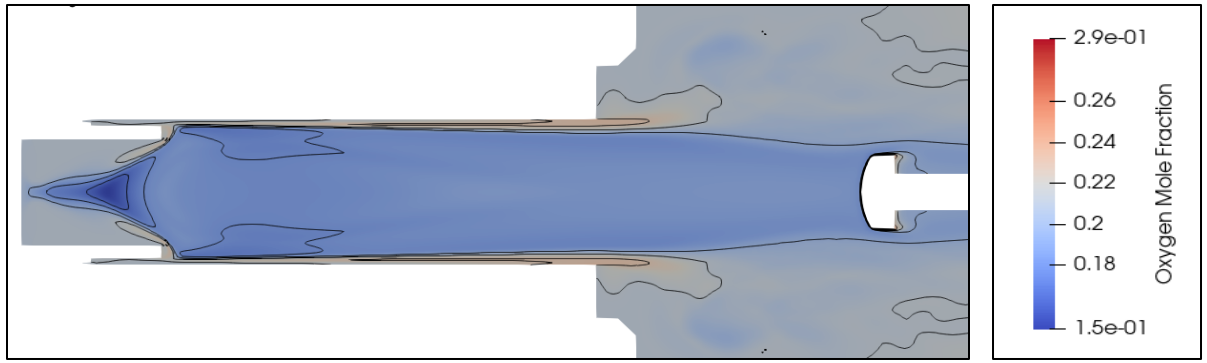


*Case: 70 mbar, 100 kW* *Oxygen Elemental Fraction*

<u>CHEMICAL NON-EQUILIBRIUM</u>

- We observe **chemical equilibrium** only outside of the torch and before the sample
- The flow is affected by **demixing**: elemental fractions of O and N diffuse inside the flow
- At standard conditions, elemental fractions of O and N are 0.21 and 0.79 respectively
- The hypothesis of chemical equilibrium is **NOT** appropriate

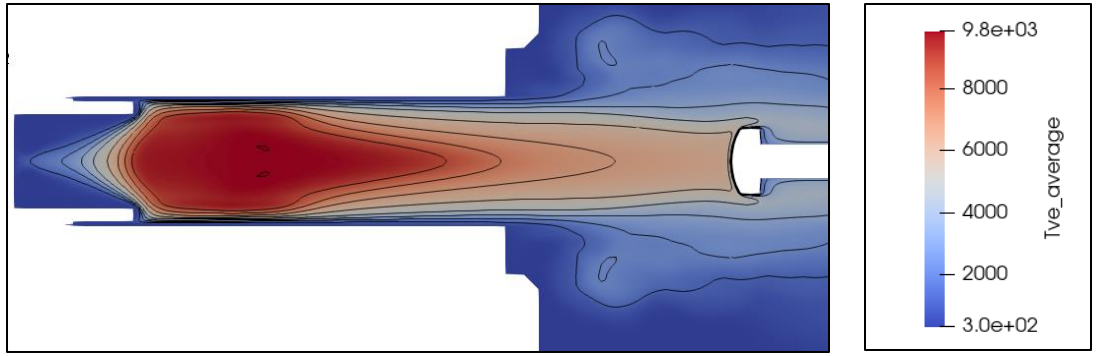


*Case: 70 mbar, 100 kW* *Vibrational Temperature*

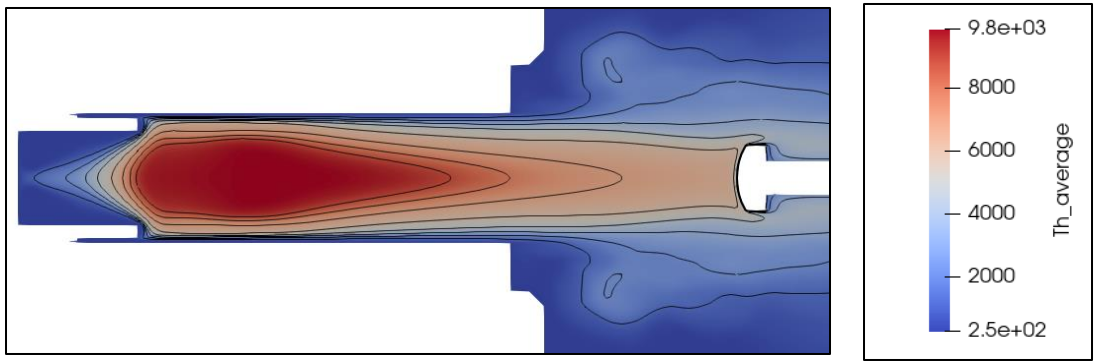


*Case: 70 mbar, 100 kW* *Translational Temperature*

<u>THERMAL NON-EQUILIBRIUM</u>

- Thermal non-equilibrium is observed inside the **torch**
- In the **chamber** thermal equilibrium is observed, while slight non-equilibrium is observed at the sample boundary layer
- Necessity to run **NLTE** full ICP simulations is justified

# Results

## FULL ICP SIMULATION RESULTS:

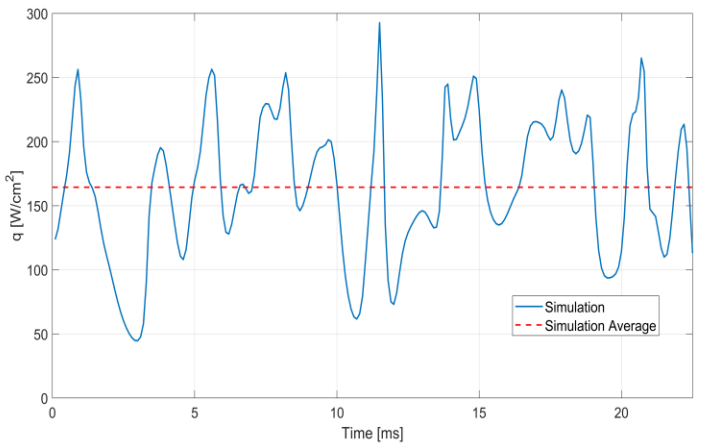


*Case: 70 mbar, 100 kW*

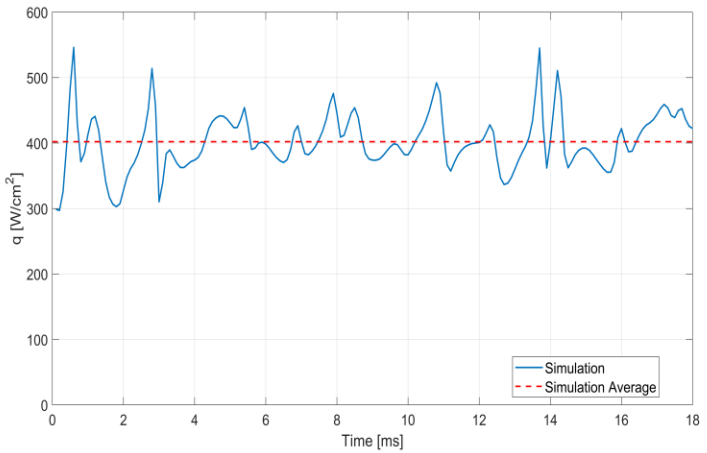


*Case: 70 mbar, 200 kW*

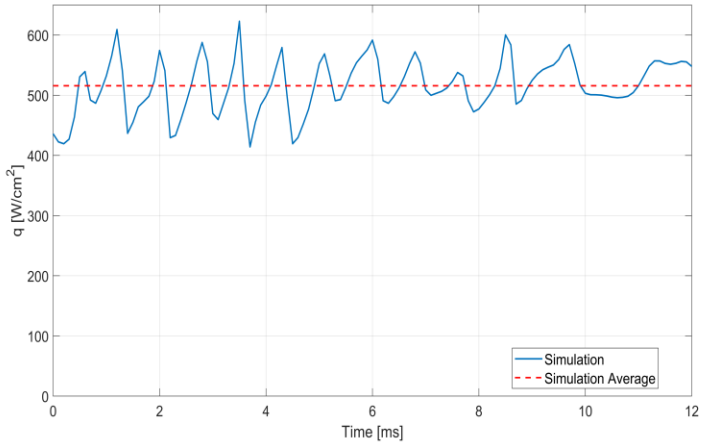


*Case: 70 mbar, 250 kW*

JET UNSTEADINESS

- From the experiments it can be seen that the jet is inherently **unsteady**
- Simulations have to be done in **time-accurate**
- Carrying out NLTE full ICP simulation in time accurate is very **computationally expensive**
- The **average** value of the full flowfield was computed
- Average **heat flux** value was extracted for comparison with experimental results
- The jet unsteadiness is decreasing at higher power

# Results

## 1D STAGNATION LINE SIMULATION RESULTS:

PROCEDURE FOR USING 1D HEGEL STAG LINE

- Consider a point in front the sample in thermodynamic equilibrium (chosen to be **1 cm from the sample**)
- Extract values of **temperature, pressure, axial velocity, and radial gradient of the radial velocity** from Full ICP 2D axisymmetric
- Use these values as **input** for the 1D code
- Run **1D HEGEL Stag Line** to obtain the heat flux with different recombination probabilities

ADVANTAGES

- The c**omputational time** is extremely low
- A wide range of simulations can be done by changing the boundary conditions or the pressure

VALIDATION

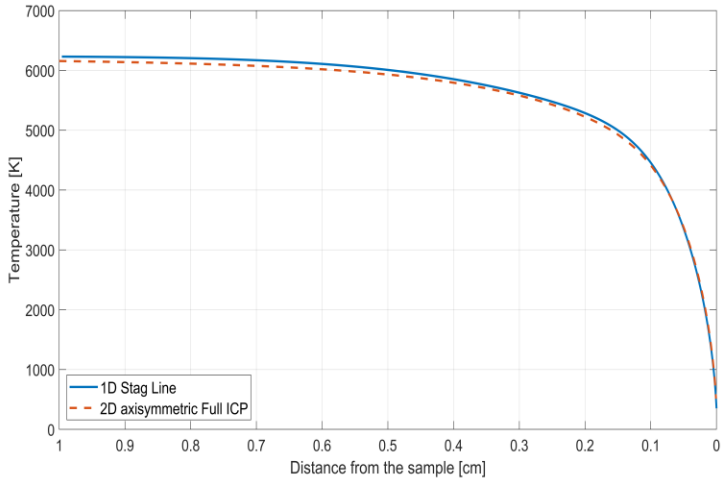


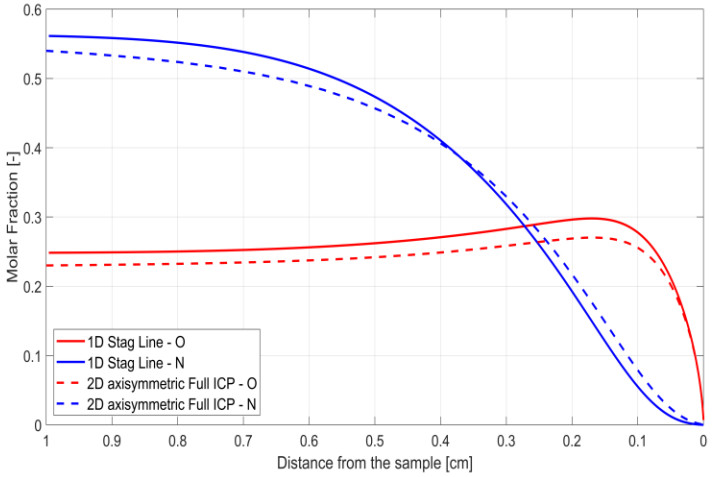


*Case: 70 mbar, 250 kW*

# Results

## MODEL VALIDATION – HEAT FLUX

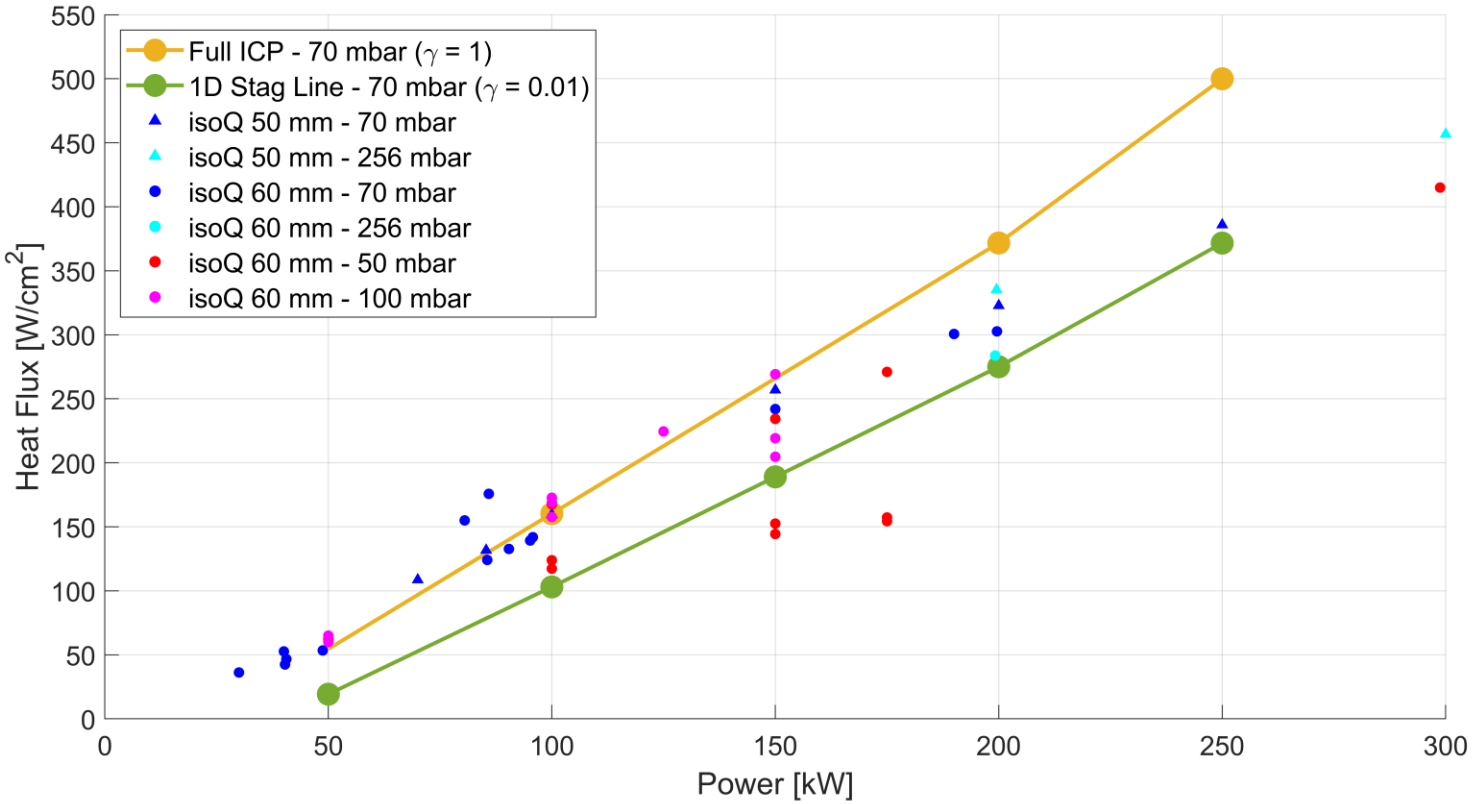


- Heat flux strongly depends on the value of **recombination probability**
- Heat flux varies **linearly** with power
- The correct recombination probability for copper is likely between 1 and 0.01
- **The trend is captured well by the model simulations, which agree within 10% or better with the experiments**

N.B. Notice how the pressure does not appreciably influence the heat flux value

*Acknowledgements to Teddy Mansfield for taking the OES measuraments, calibrating, and doing the fits*
*Brandis, Aaron M., and Brett A. Cruden. NEQAIR v15. 0 release notes: nonequilibrium and equilibrium radiative transport and spectra program. No. ARC-E-DAA-TN72963. 2019.*

# Methodology

## TEMPERATURES FROM OES:

In order to use the OES measurements for validation, **temperatures** have to be extracted from the OES spectrum

This can be achieved by producing a synthetic spectrum using the radiation software **NEQAIR**:

- Consider a single point radiation source (0D model)
- Assume local thermodynamic equilibrium
- Assume a Boltzmann distribution
- Line by line integration

Given these assumptions, a synthetic spectra, represented by **normalized intensity** as a function of the wavelength, is produced

By using an **optimization procedure**, the temperature that makes the OES spectrum and the code-generated spectrum match, is extracted

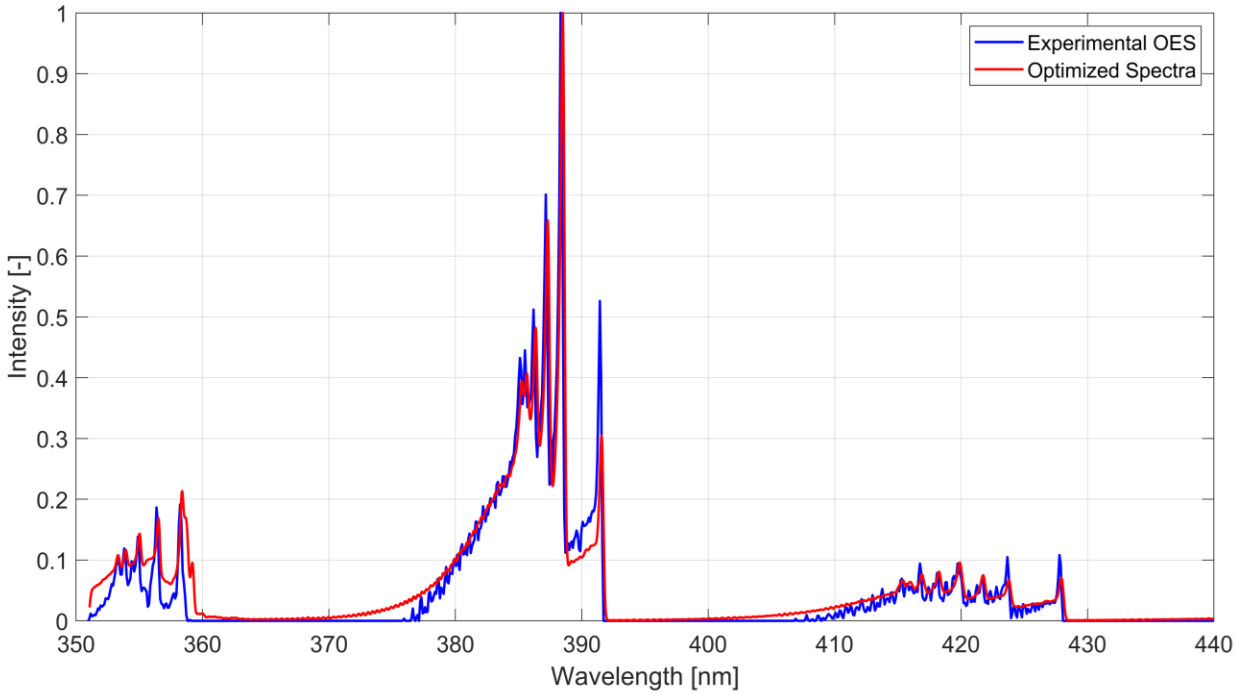


*Example fit done with MURP*

# Methodology

## RADIATIVE TRANSPORT:

OES measurements are represented by intensities measured at the instrument lens placed at the end of a **Line Of Sight (LOS)** perpendicular to the jet

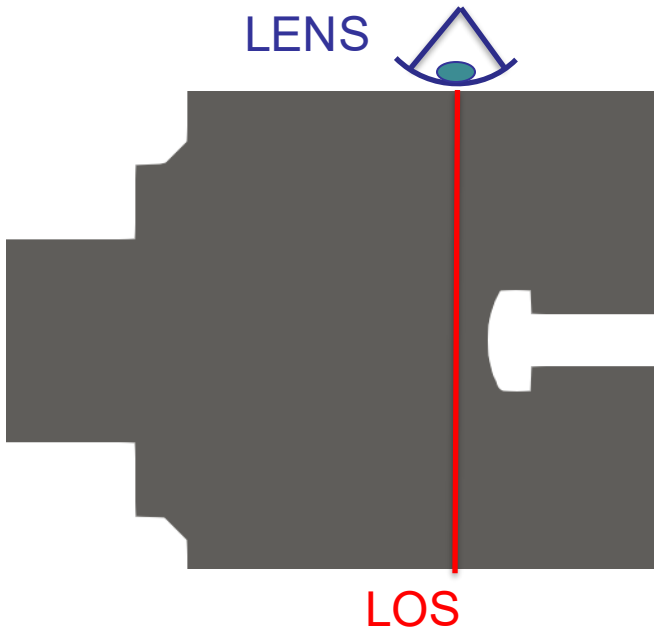


To allow a fair comparison, the same LOS radiative transport at the lens was computed from the **simulation results**

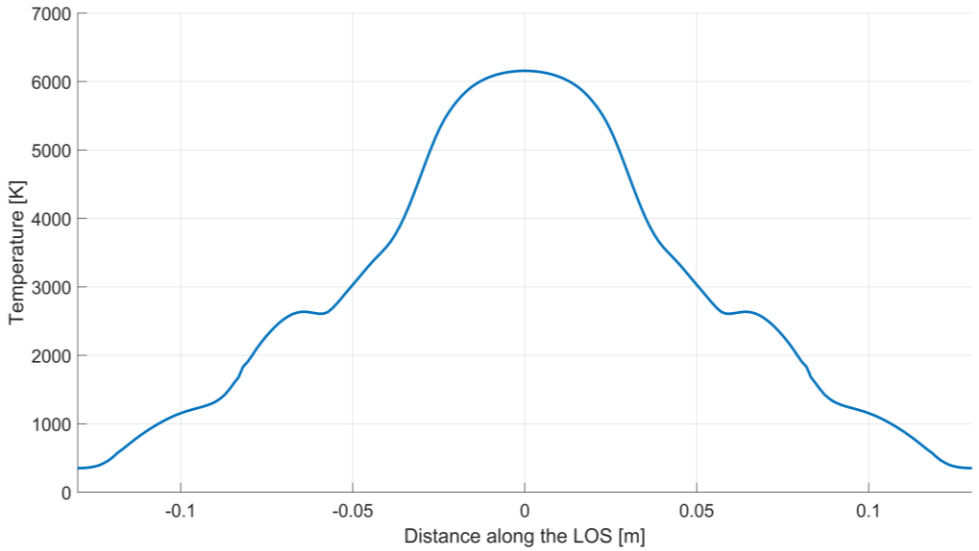


*Example of radial profile along the LOS*

1. Extract the radial simulation profile along the **LOS**
2. **Sample** the profile with 200 evenly spaced points
3. Compute the **LOS path-integrated** spectrum using **MURP**
4. **Fit** the spectrum using NEQAIR (in the same way as for OES)

We are reproducing what the OES spectrometer does in reality, also in the simulations

*Acknowledgements to Teddy Mansfield for taking the OES measurements, calibrating, and doing the fits*

# Results

## MODEL VALIDATION – TEMPERATURES

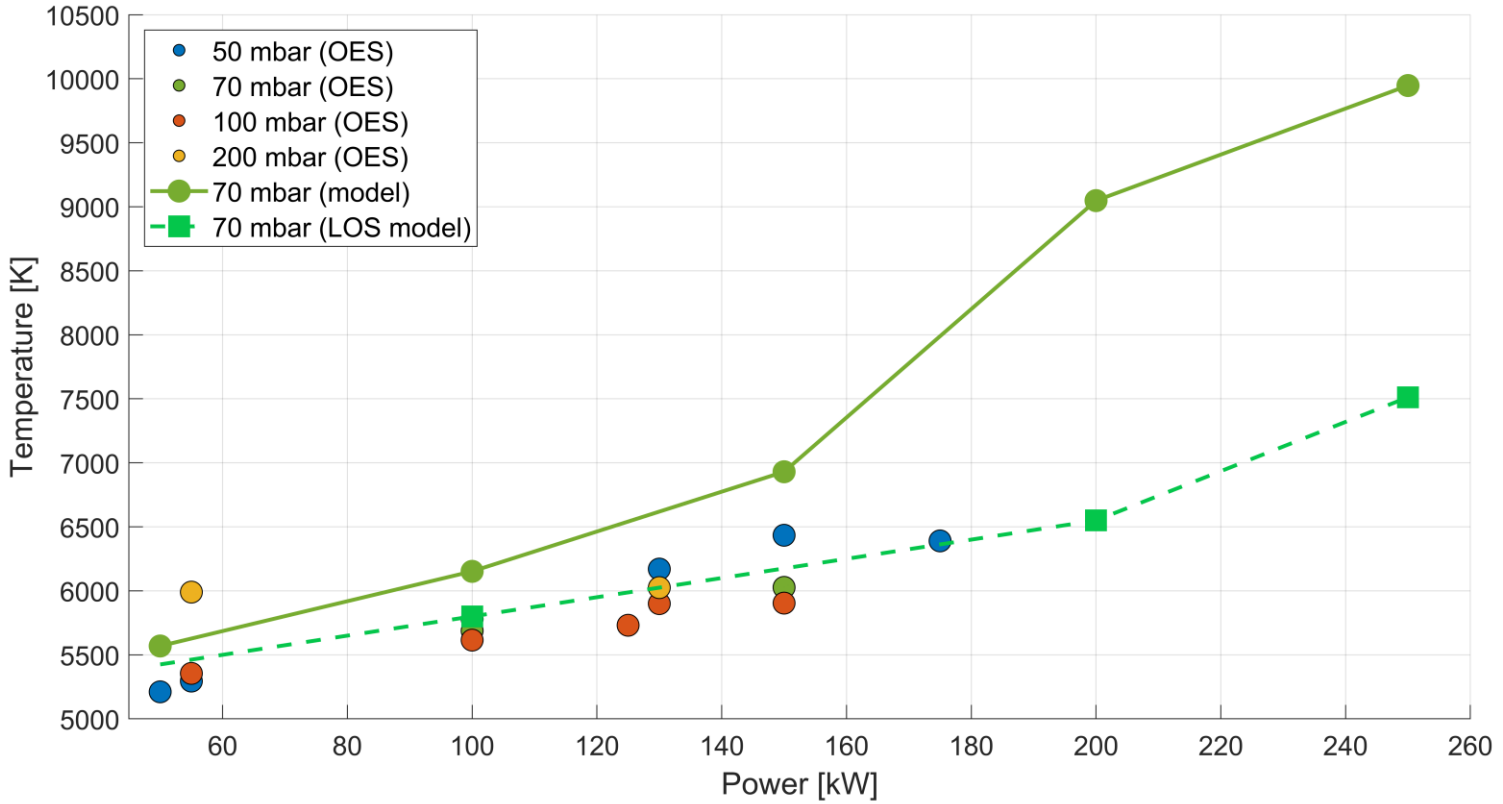


- **OES temperature** spectrum should be lower than the jet centerline value
- The path-integrated spectrum (LOS) of the **model simulations** was computed for a more direct comparison
- **Simulations (LOS) and OES agree within 10% or better**
- **Radiation** losses should also be included

N.B. The temperatures labeled *model* are taken at the boundary layer edge along the stagnation line

# Results

## FLIGHT EXTRAPOLATION - VELOCITY

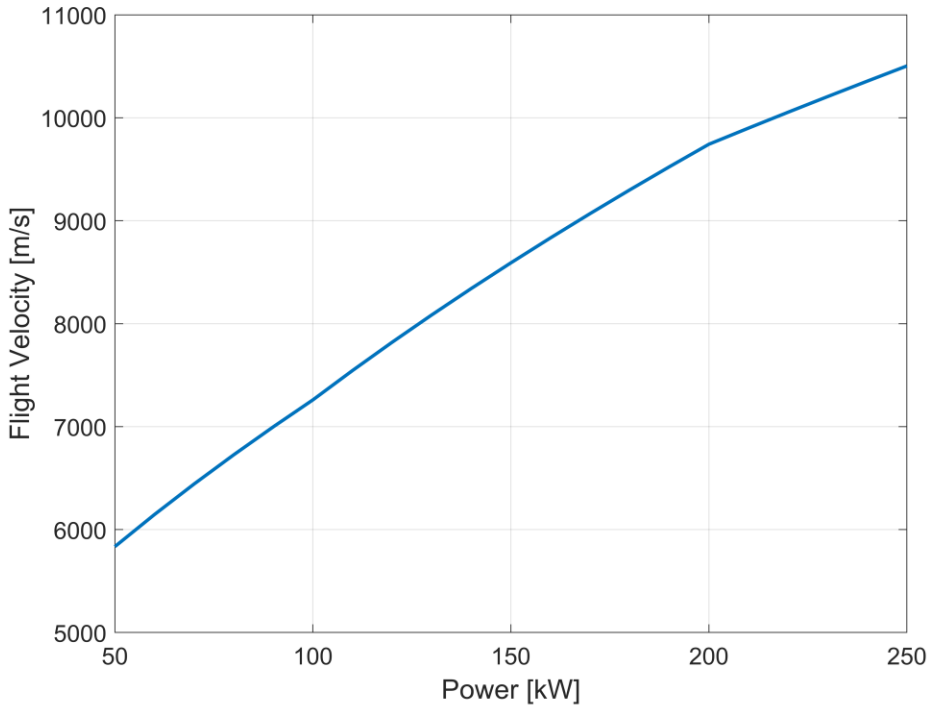


$$V_{flight} = \sqrt{2H^{e}_{facility}}$$

- The **enthalpy** is assumed to be constant with pressure (or negligibly changing)
- By matching the in-flight and ground-test total enthalpy, a formula for the **flight velocity** is obtained
- Velocity only varies with **power**
- The power range used corresponds to flight velocities in the range of **past re-entry missions** (e.g., Apollo, Dragon)

# Results

## FLIGHT EXTRAPOLATION - ALTITUDE

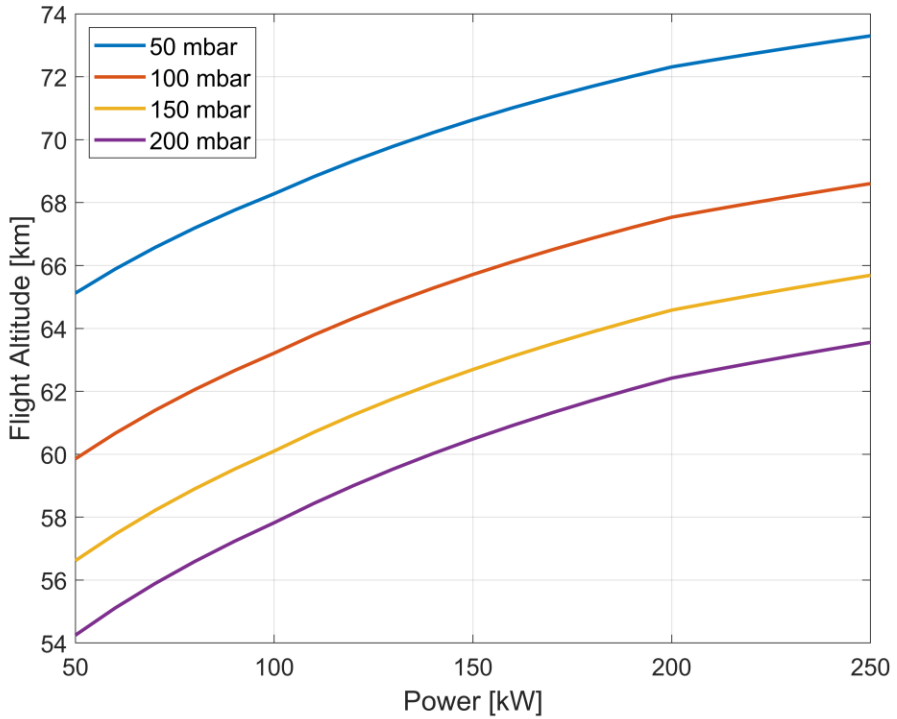


$$\rho_{flight} = \frac{P^e_{facility}}{2H^e_{facility}}$$

- By matching the in-flight and ground test total pressure, a formula for the **flight density** is obtained
- Using the **standard atmospheric model**, we can determine the altitude corresponding to the given density
- Flight altitude depends on both facility power and pressure, in a coupled way
- The extrapolated altitudes fall within the **continuum flow regime** and lie in a range of interest for past missions

# Conclusions

## ACHIEVEMENTS:

- Used a state-of-the-art multi-physics computational model (**HEGEL** + **PLATO** + **FLUX**) to accurately describe the flowfield inside an ICP facility
- Provided **model validation** through comparison of heat flux measurements, and temperatures obtained by fitting path-integrated LOS spectra using radiation codes (MURP and NEQAIR)
- Performed **flight extrapolation** of the testing conditions using the model simulations

## FUTURE WORK:

- Widen the pressure correlation range through **1D stagnation line simulations** and by performing additional **full ICP simulations**
- Perform and analyze **in-flight radius** extrapolation from the velocity gradient
- Repeat the validation and extrapolation procedure for a different gas, specifically **carbon dioxide**

# Introduction

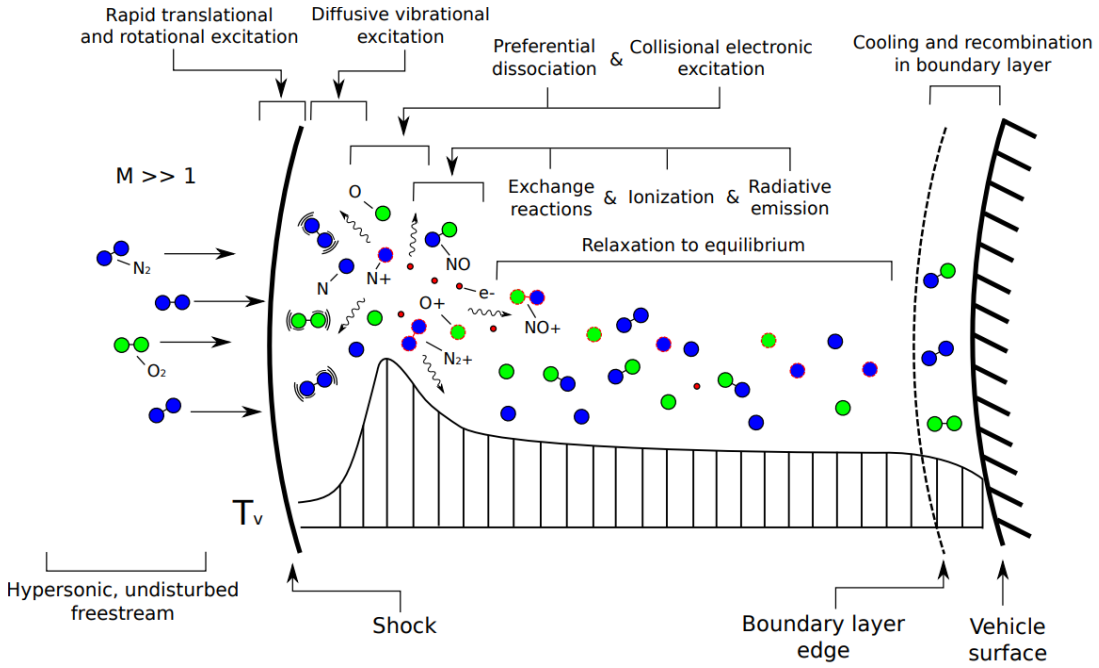


*Potter, Daniel. "Modelling of radiating shock layers for atmospheric entry at Earth and Mars." Scientaa AC Abore, s4029188 phD Thesis (2011)*

Quickly after the shock, the particles collide to move towards **chemical and thermal equilibrium**; this process is called relaxation

**Translational** and **rotational** energy modes equilibrate quickly with each other; **vibrational** and **electronic** come after, due to less efficient energy transfer

At thermal equilibrium, all the energy modes are at the same temperature. At chemical equilibrium, all the species' concentrations are constant

Close to the wall, heat transfer with the wall starts to create large gradients in the flow, which lead to **thermodynamic non-equilibrium**

# Physical Modeling:

## PLASMA FIELD

### TRANSPORT:

- Transport properties and diffusive fluxes are computed using the **first-order Chapman–Enskog** method for partially ionized plasmas
- Shear stresses and conductive heat fluxes are modeled using **Newton's** and **Fourier's laws**, respectively
- Diffusion velocities are computed from the **Stefan–Maxwell** equations

### THERMODYNAMICS:

- Gas pressures follow **Dalton's Law**; $p = p_h + p_e$
- Internal energy of **free electrons** includes only the translation contribution
- Internal energy of **atoms** include translational, electronic, and formation contributions
- Internal energy of **molecules** includes translational, rotational, vibrational, electronic, and formation contributions

# Physical Modeling:

## ELECTROMAGNETIC FIELD

Described by **Maxwell's equations**, with the following simplifying assumptions:

- Low-frequency approximation; frequency of inductive source is lower than plasma frequency
- Low magnetic Reynolds number ($R_m$ << 1): plasma motion cannot convect ***B***
- Ambipolar diffusion; no current in the poloidal plane

Maxwell's equations that are obtained:

$$\nabla \times \nabla \times \tilde{E} + i\mu\sigma\omega\tilde{E} = -i\mu\omega\tilde{J}_s$$

Assuming a monochromatic time dependency of ***B*** and ***E***, it's possible to express ***B*** as a function of ***E*** through **Faraday's Law**:

$$\tilde{B}_{re} = -\frac{1}{\omega}\nabla \times \tilde{E}_{im} \quad and \quad \tilde{B}_{im} = -\frac{1}{\omega}\nabla \times \tilde{E}_{re}$$

**Lorentz force** and **Joule heating** are averaged over the fast electromagnetic scale, yielding:

$$\langle \mathbf{J} \times \mathbf{B} \rangle = \frac{1}{2}\frac{\sigma}{\omega}\left[\tilde{\mathbf{E}} \times (i\nabla \times \tilde{\mathbf{E}})^*\right]$$

$$\langle \mathbf{J} \cdot \mathbf{E} \rangle = \frac{1}{2}\sigma\tilde{\mathbf{E}} \cdot \tilde{\mathbf{E}}^*$$

# Physical Modeling

## STAGNATION LINE 1D FLOW

- Methodology proposed by **Klomfass and Müller** for stagnation line flow
- Quasi-one-dimensional approximation of the **stagnation streamline**
- The resulting set of simplified equations is called the **Dimensionally Reduced Navier–Stokes Equations (DRNSE)**

Equations are obtained by:

1. Expressing the Navier-Stokes equations in **spherical coordinates**
2. Applying separation of variables to a set of flow quantities
3. Representing these flow variables as products of unknown functions of the radial coordinate and empirically prescribed functions of the **angular coordinate**
4. Performing analytical differentiation of functions of angular coordinates, leading to the derivation of the DRNSE

$$\bar{\mathbf{u}}_{,t} + \bar{\mathbf{F}}^I_{,r} + \bar{\mathbf{F}}^V_{,r} + \left(\bar{\mathbf{G}}^I + \bar{\mathbf{G}}^V\right) r^{-1} = \mathbf{S},$$

$$\bar{\mathbf{u}} = \begin{bmatrix} \rho_1 \\ \vdots \\ \rho_N \\ \rho\bar{v}_r \\ \rho\bar{v}_\theta \\ \rho E \end{bmatrix}, \quad \bar{\mathbf{F}}^I = \begin{bmatrix} \rho_1\bar{v}_r \\ \vdots \\ \rho_N\bar{v}_r \\ \rho\bar{v}_r^2 + p \\ \rho\bar{v}_r\bar{v}_\theta \\ \rho\bar{v}_r H \end{bmatrix}, \quad \bar{\mathbf{F}}^V = \begin{bmatrix} j_{r1} \\ \vdots \\ j_{rN} \\ \tau_{rr} \\ \tau_{r\theta} \\ q_r + \tau_{rr}\bar{v}_r \end{bmatrix},$$

$$\bar{\mathbf{G}}^I = \begin{bmatrix} 2\rho_1(\bar{v}_r + \bar{v}_\theta) \\ \vdots \\ 2\rho_N(\bar{v}_r + \bar{v}_\theta) \\ 2\rho\bar{v}_r(\bar{v}_r + \bar{v}_\theta) \\ 3\rho\bar{v}_\theta(\bar{v}_r + \bar{v}_\theta) - 2\bar{p} \\ 2\rho H(\bar{v}_r + \bar{v}_\theta) \end{bmatrix}, \quad \bar{\mathbf{G}}^V = \begin{bmatrix} 2j_{r1} \\ \vdots \\ 2j_{rN} \\ 2(\tau_{rr} - \bar{\tau}_{\theta\theta} + \bar{\tau}_{r\theta}) \\ -\bar{\tau}_{\theta\theta} + 3\bar{\tau}_{r\theta} \\ 2(q_r + \bar{\tau}_{rr}\bar{v}_r + \bar{\tau}_{r\theta}\bar{v}_r + \bar{\tau}_{\theta\theta}\bar{v}_\theta) \end{bmatrix}$$